

Understanding Key NaCMC Properties to Optimize Electrodes and Battery Performance

Noah Keim,* Andreas Weber, Marcus Müller, Ulrike Kaufmann, Werner Bauer, Oliver Petermann, Roland Bayer, and Helmut Ehrenberg

This study examines the effects of sodium carboxymethyl cellulose (NaCMC) on the performance of graphite anodes in lithium-ion batteries, focusing on variations in degrees of substitution (DS), molecular weights (MW), and gel particles. The results indicate that the best electrochemical performance is achieved by balancing the residual water content introduced by NaCMC while maintaining the anode's volume resistivity. A NaCMC with a low molecular weight and DS of 0.7 shows the best results for this particular formulation. An impurity (in batteries yet unreported) in NaCMC is also reported that significantly impacts electrochemical performance, called gel particles. By reducing the gel particles, cell performance is enhanced by 5%, without further optimization of the formulation. It is highlighted that both DS and MW influence electrode properties. A decrease in DS enhances adhesion but negatively affects volume resistivity. Increasing the MW improves adhesive strength and reduces interfacial resistivity due to greater chain entanglements. Higher gel particle levels negatively impact electrode properties, making low-gel NaCMC more effective for better adhesion and resistance. Water retention in electrodes again is influenced by both DS and MW. Higher DS leads to increased water retention due to greater hydrophilicity, while high MW contributes to this effect through enhanced entanglements.

1. Introduction

In recent years, interest in high energy density storage has surged, driven by the need for high-power and high-capacity batteries.^[1] Especially, electric vehicle batteries require low weight

and high energy density due to space constraints. Currently, only lithium-ion batteries (LIBs) meet these needs and the main research focuses to fulfil the demand usually is on the active material side.

Hence, the binders are often overlooked despite playing a crucial role in battery functionality by creating a suitable environment for the active material, while also providing mechanical stability for the electrode.^[2] Additionally, the binder must function as a proper dispersant during slurry preparation, while also demonstrating high electrochemical stability and influencing the formation of the solid electrolyte interphase (SEI), which is considered a protective layer that forms on the anode surface during cycling by decomposing the electrolyte's salt and solvents. The electrochemical stability is especially important for full cells, because losing any amount of lithium ions to side reactions drastically impacts longevity by capacity fading.

Currently, polyvinylidene fluoride (PVDF) is used for its stability and adhesion properties in cathodes.^[3] However, the need to replace PVDF arises from the use of harmful N-methyl-2-pyrrolidone as a solvent, which requires high temperatures to dry electrodes and poses as a risk to work safety. For anodes, water-soluble binders, like sodium carboxymethyl cellulose (NaCMC), are already being used at industrial scale.^[4] It is a natural, biodegradable polymer derived from cellulose. NaCMC's degree of substitution (DS) and molecular weight (MW) are known key factors influencing its performance, though their impact on electrode properties and the connection to cell performance needs further understanding.^[4,5] Finally, despite growing interest, potential side products during NaCMC synthesis, referred to as gel particles, have been overlooked due to their minimal presence. Croscarmellose sodium is one possible side product which occurs during the synthesis of NaCMC. First, NaCMC is synthesized by reacting cellulose with monochloroacetic acid in the presence of sodium hydroxide, resulting in carboxymethylation of the cellulose backbone. Excess monochloroacetate presents during the synthesis of hydrolyses to glycolic acid. Some of the hydroxyl moieties then react with adjacent NaCMC chains, as the glycolic acid allows for acidic dehydration.^[6] This leads NaCMC to crosslink via esterification, see Figure 1.

N. Keim, A. Weber, M. Müller, U. Kaufmann, W. Bauer, H. Ehrenberg
Institute for Applied Materials (IAM)
Karlsruhe Institute of Technology (KIT)
Hermann-von-Helmholtz-Platz 1
D-76144 Eggenstein-Leopoldshafen, Germany
E-mail: noah.keim@kit.edu

O. Petermann, R. Bayer
IFF N&H Germany GmbH & Co. KG
August-Wolff-Strasse 13, D-29699 Walsrode-Bomlitz, Germany

The ORCID identification number(s) for the author(s) of this article can be found under <https://doi.org/10.1002/aesr.202400364>.

© 2025 The Author(s). Advanced Energy and Sustainability Research published by Wiley-VCH GmbH. This is an open access article under the terms of the Creative Commons Attribution License, which permits use, distribution and reproduction in any medium, provided the original work is properly cited.

DOI: 10.1002/aesr.202400364

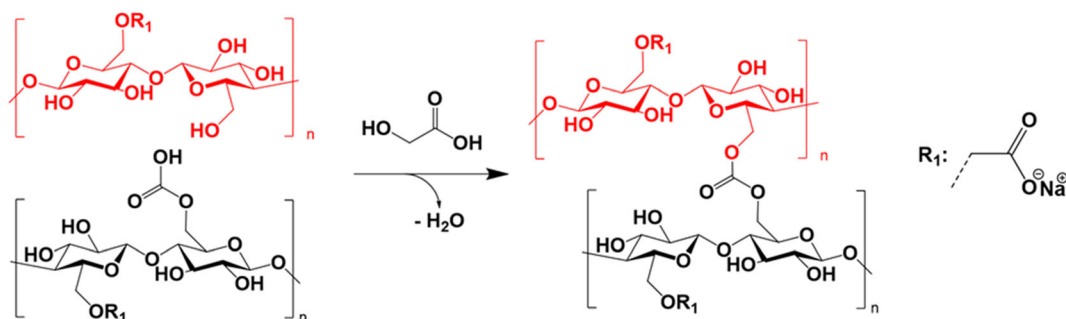


Figure 1. Schematic reaction of possible gel particles (croscarmellose sodium) from NaCMC.^[6]

This report outlines the investigation into how different polymer properties and varying amounts of gel particles can affect both electrodes and cell performance. The objective of this research is to provide valuable insights into optimizing the composition of LIB electrodes for enhanced energy storage and cycling stability.

2. Results and Discussion

2.1. Electrode Properties

2.1.1. Influence of DS and MW

The key electrode properties of electrodes include their resistivity and the adhesive strength to the current collector. Figure 2 depicts the results of the adhesion strength and volume

resistivity measurement and reveals a significant impact of both the DS and the MW of the NaCMC.

By decreasing the number of substituents from CMC_{0.9, low MW} to CMC_{0.5, low MW}, the adhesion strength increases from 25.1 N m⁻¹ for CMC_{0.9, low MW} by 18% to 29.6 N m⁻¹ for CMC_{0.5, low MW}. The increase in adhesion strength for a lower DS is also valid for high molecular weights, and therefore not solely dependent on the increase in polymer length. Independent of the DS, all high MW NaCMCs show superior adhesive results in comparison to their counterpart.^[7] Still, the relative increase at high MWs for CMC_{0.9, high MW} with 29.5 up to 36.2 N m⁻¹ for CMC_{0.5, high MW} equals 22% and shows that the DS influences the adhesive strength for both high and low MW NaCMCs.

In contrast, the resistivity of the electrodes only seems to be significantly impacted by the DS for the low MWs as the volume

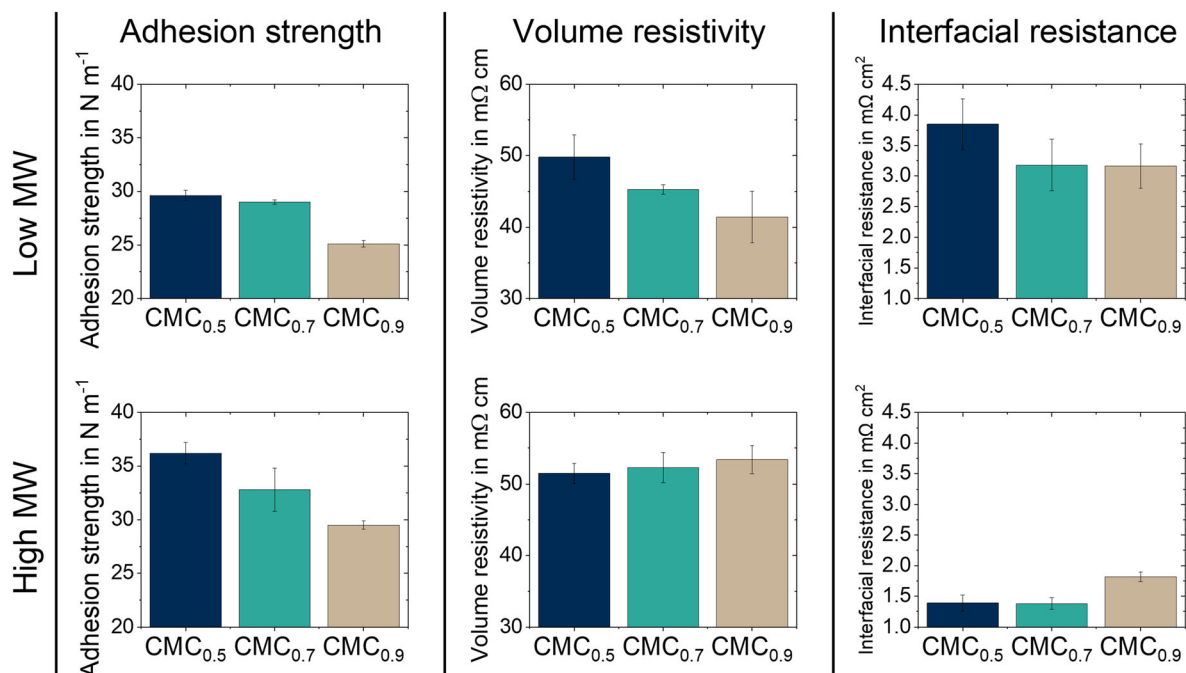


Figure 2. Summary for adhesion strength, volume resistivity, and interfacial resistance of graphite anodes containing varying NaCMC in regards of DS and MW. Upper row depicts low MW NaCMCs, while the lower row depicts the high MW NaCMCs. NaCMCs with the same DS are depicted in the same color.

resistivity increases from $41.4 \Omega \text{ cm}$ for $\text{CMC}_{0.9, \text{ low MW}}$ to $49.8 \Omega \text{ cm}$ for $\text{CMC}_{0.5, \text{ low MW}}$. Increasing the MW leads to an overall increase of the volume resistivity independent of the DS, as shown by $\text{CMC}_{0.9, \text{ low MW}}$ increasing from 41.4 to $53.4 \Omega \text{ cm}$ for $\text{CMC}_{0.9, \text{ high MW}}$ with a high MW.

As opposed to the increase dependent on the DS shown for the adhesion, there is no similar effect noticeable for high MW NaCMC regarding volume resistivity. Additionally, the trend regarding the interfacial resistance between low and high MWs deviates as well. This is attributed to two factors gaining relevancy due to an increase in chain length: less mobile binder and more entanglements due to higher chain length.

The increase in MW leads to a decreasing amount of smaller and more mobile NaCMC polymer chains in the sample. This equals less free short-chain NaCMC, which is less likely to be adsorbed on the surface of the graphite and carbon black (CB) in comparison to longer polymer chains.^[8] Therefore, the current collector is less prone to be covered in free short NaCMC polymer chains, which are unlikely to interact with the carbon-binder-domain (CBD).^[9] The CBD is considered a conductive network formed by carbon particles and binder, facilitating electron transport and mechanical stability within the electrode.^[10] Higher MW NaCMC has longer polymer chains. This increase allows free binder with higher MW to adhere to the copper collector and styrene-butadiene rubber (SBR) while also creating entanglements with other polymer chains. Therefore, high MW NaCMCs increase the number of contact points of the CBD to the current collector while reducing the interfacial resistance. This is also in good agreement with the adhesion results. Furthermore, lower MW NaCMCs result in fewer chain entanglements, which could result in a more significant binder migration during the drying process. This pronounced binder migration has been associated with higher interfacial resistance.^[11] This observation aligns with the measured electrical resistance, as all low MW NaCMCs consistently exhibit relatively higher interfacial resistance compared to their higher MW counterparts.

The water retention of graphite electrodes, which were dried according to the cell manufacturing procedure, was characterized and is illustrated in **Figure 3**.

Figure 3 shows that the water retention increases with increasing DS and is even more pronounced for high MW. Water residue in the anodes for a low DS and a low MW is the lowest, with 75 ppm for $\text{CMC}_{0.5, \text{ low MW}}$. The residual content for $\text{CMC}_{0.9, \text{ low MW}}$ with 194 ppm water is significantly higher, equaling an increase of 150%. We attributed the increase of water retention to higher DS, which leads to a higher hydrophilicity of the NaCMC.^[12]

By increasing the MW, the same dependency on the amount of carboxyl moieties is still present as the highest DS in $\text{CMC}_{0.9, \text{ high MW}}$ leads to the highest water retention. $\text{CMC}_{0.5, \text{ high MW}}$ shows the lowest amount of residual water in the anode with 360 ppm of water. Interestingly, the difference in between $\text{CMC}_{0.5, \text{ high MW}}$ and $\text{CMC}_{0.7, \text{ high MW}}$ is significantly larger than for the low MW. Compared to the low MW, the water content multiplied for all electrodes containing higher MW NaCMCs. This is due to the increase in MW resulting in a growing number of entanglements, as already implied by the adhesion results. Those entanglements lead to water being trapped

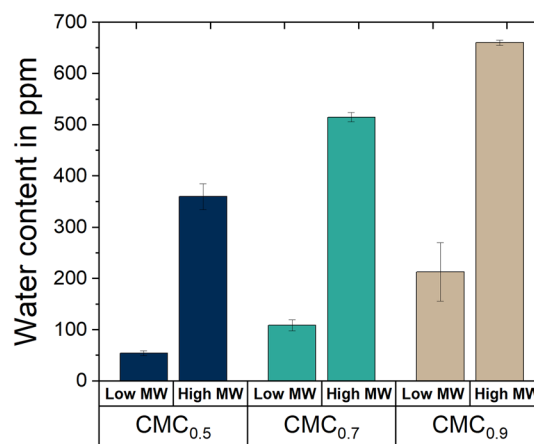


Figure 3. Water retention determined via Karl–Fischer for graphite electrodes after 16 h of drying at 130°C containing varying NaCMCs.

in between the interacting polymer chains, which in term allows for a better water retention.^[7a]

2.1.2. Influence of Gel Particles

For this investigation a new batch of copper foil from a new supplier was used. Therefore, despite using the same NaCMC, different results were obtained (Figure 2: $\text{CMC}_{0.7, \text{ low MW}}$ and **Figure 4:** Gel_{10}) regarding the interface between current collector and electrode layer (adhesion strength, interfacial resistance). By controlling the synthesis, the amount of gel particles is reduced. As shown above, a variation of the NaCMC polymer significantly impacts the anode properties. While unexpected, it is also evident for the gel particles, despite contributing only a fraction of the NaCMC, see Figure 4.

The adhesion increases from 11.3 to 18.7 N m^{-1} , while the interfacial resistance reduces from $2.2 \text{ m}\Omega \text{ cm}^2$ for Gel_{250} to $1.4 \text{ m}\Omega \text{ cm}^2$ for Gel_{10} . Similar results can be seen for the volume resistivity, which also decreases with lower contents of gel particles. The decrease in both the interfacial resistance and volume resistivity indicates a better dispersion of the carbon additive during the processing for Gel_{10} in comparison to Gel_{250} . This is further underlined by the increase in adhesion, which would represent a higher number of contacts between the copper collector and the CBD. Therefore, by creating a higher grade of NaCMC, it is possible to improve the electrode properties significantly, without further optimizing the electrode composition.

2.2. Electrochemical Characterization

2.2.1. Impact of DS and MW

The results of the rate capability and the adjoining long-term cycling tests for electrodes containing NaCMC with varying DS and low MW are summarized in **Figure 5**.

$\text{CMC}_{0.7, \text{ low MW}}$ shows the highest capacities, followed by $\text{CMC}_{0.9, \text{ low MW}}$ with $\text{CMC}_{0.5, \text{ low MW}}$ showing the lowest performance for the low MW DS variation. While all electrodes independent of NaCMC perform well for low discharging rates, the

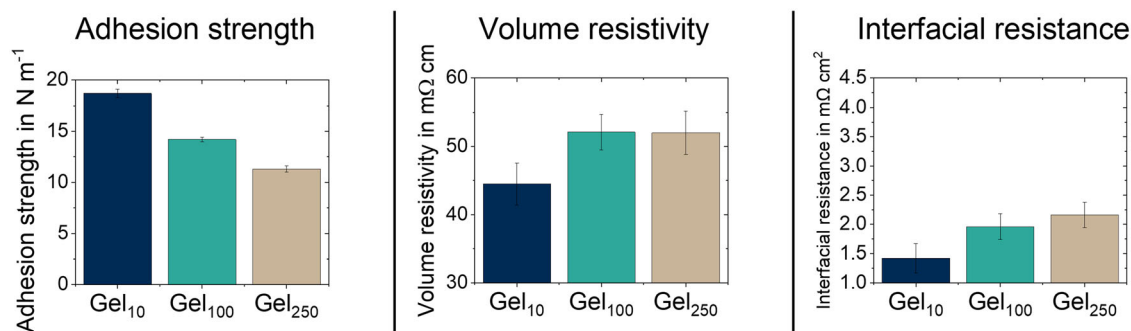


Figure 4. Electrode properties of graphite anodes containing NaCMC with a varying amount of gel particles.

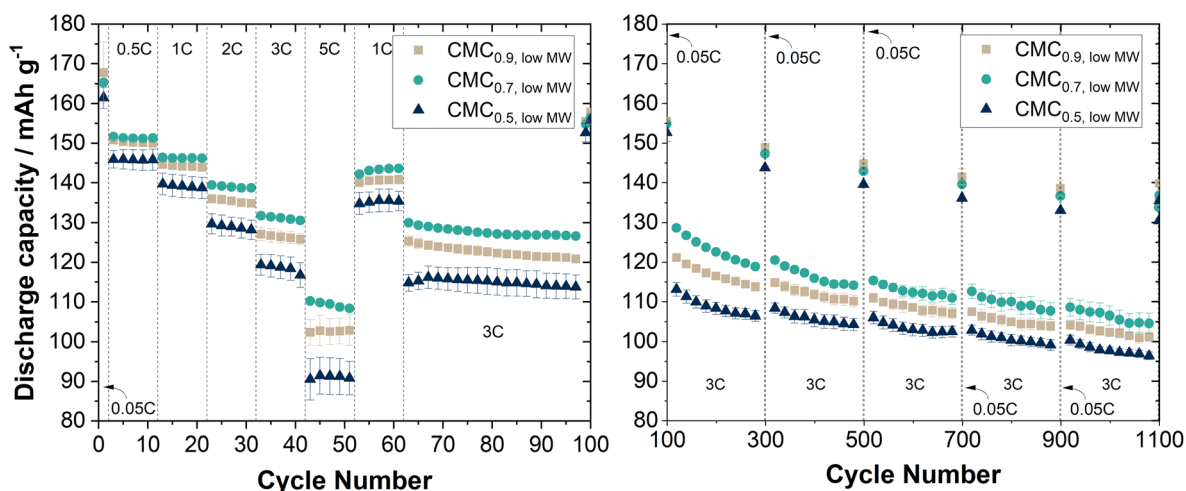


Figure 5. Rate test and long-term cycling for electrodes containing NaCMC with low MW and varying DS. For every 200 cycles, there are two 0.05 C cycles during long-term cycling. For the sake of visibility, only every second value is shown in the rate test and every 20th for the long-term cycling.

disparity in cell performance increases, the more the cell gets strained at higher discharging rates. CMC_{0.9, low MW} was found to exhibit poor rate capability test performance, which is attributed to the increased residual water content. This correlation aligns with previous reports who demonstrated that higher residual water leads to more pronounced parasitic reactions.^[13] These side reactions consume lithium ions and electrolyte creating a less mechanically stable SEI and reduced electrolyte conductivity, thereby negatively impacting the overall cell performance.

Accordingly, NaCMCs with a lower DS were anticipated to perform better due to their reduced water retention suggesting a decrease in parasitic reactions and improved rate capability. CMC_{0.7, low MW} showed improved cell performance over CMC_{0.9, low MW}, increasing capacity by reducing the residual water content and the related parasitic side reactions. Instead of further improving, CMC_{0.5, low MW} exhibited worse performance compared to its higher DS counterparts. This is especially apparent at higher discharging rates. The electrical resistance in electrodes with CMC_{0.5, low MW} was significantly higher, see Figure 2. By increasing the resistance, an increased polarization is expected leading to overall worsened cell performance, especially at higher discharging rates.^[14] This higher resistance overshadowed probable benefits gained from the reduced water content ultimately leading to a worse performance.

The findings regarding DS have demonstrated how variations in water retention and resistance directly affect the electrochemical performance of anodes with different NaCMC binders. Building on this, results regarding NaCMCs with higher MW further explore the role of the NaCMCs influence on the electrochemical performance. This progression from DS to MW analysis provides a comprehensive understanding of the key electrode properties influenced by NaCMC. By also applying the aforementioned analysis techniques, regarding water retention and resistance, to high MW NaCMC samples, we observe similar performance issues, see Figure 6. As reference, the best performing NaCMC for the low MW CMC_{0.7, low MW} is displayed as well.

The increase of MW leads to the cell performance being almost indistinguishable with CMC_{0.9, high MW} showing similar results to CMC_{0.7, high MW} while CMC_{0.5, high MW} is slightly worse than both. Nonetheless, all high MW NaCMCs show inferior cell performance in comparison to their low MW equivalent. This is attributed to the increase in water retention. As previously mentioned, it leads to more parasitic side reactions decreasing the amount of available lithium ions and worsening the ionic conductivity of the electrolyte.^[13] The benefit of lower DS, being reduced water retention, is still present in low DS high MW samples like CMC_{0.5, high MW}. While still noticeable, it is less pronounced due to the significant impact of the increased number

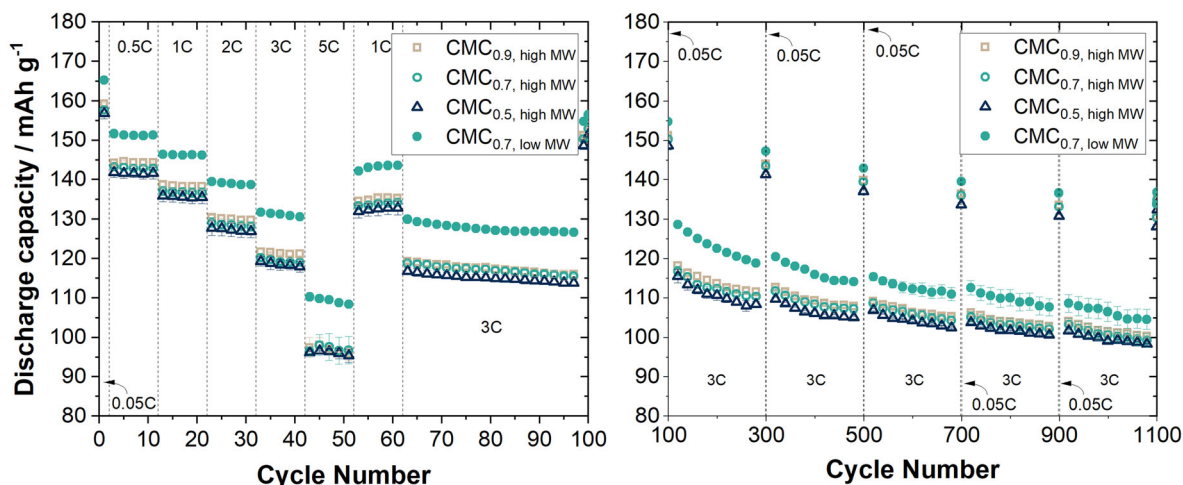


Figure 6. Rate test and long-term cycling for electrodes containing NaCMC with high MW and varying DS. As reference $\text{CMC}_{0.7, \text{low MW}}$ is used for comparison. For every 200 cycles, there are two 0.05 C cycles during long-term cycling. For the sake of visibility, only every second value is shown in the rate test and every 20th for the long-term cycling.

of entanglements on the water retention. Therefore, despite the same volume resistivity and lower water content in dried anodes containing $\text{CMC}_{0.5, \text{high MW}}$ compared to $\text{CMC}_{0.7, \text{high MW}}$ and $\text{CMC}_{0.9, \text{high MW}}$, there is no increase in the cell performance noticeable.

2.2.2. Impact of Gel Particles

Electrochemical characterization was also conducted for varying amounts of gel particles in the NaCMC, see **Figure 7**. The varying cell performance shows that electrodes with less gel particles outperform those with higher numbers of gel particles. This correlation between gel content and electrode performance highlights the impact that this small amount of side product has.

Similar to the previously shown cell results, as the discharge rate increases, the disparities between different gel particle levels

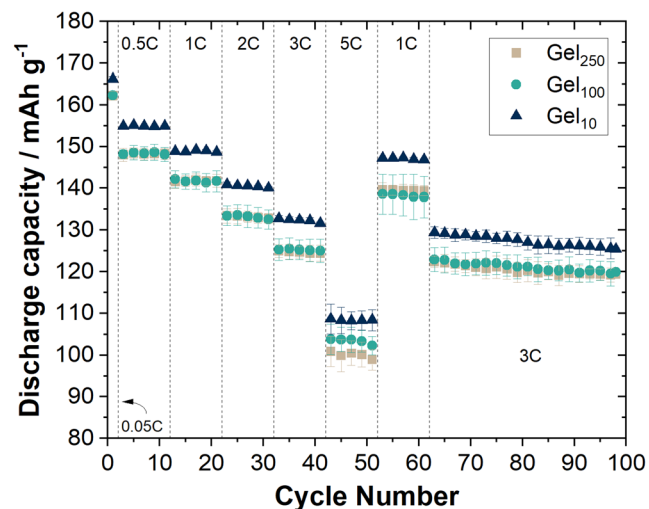


Figure 7. Rate test for varying gel particle content in the electrodes. For the sake of visibility, only every second value is shown.

become more pronounced leading to an increase of up to 5% of capacity for low gel particles. Due to Gel_{10} showing a decrease of 14% in volume resistivity, the better conductivity leads to better performance in the rate capability test. The long-term cycling provides no further insights. The cells were built as coin cells and the limited stability of these cells overshadowed the impact of the gel particles on the effects of long-term cycling.^[15]

3. Conclusion

In summary, the performance of NaCMC-based electrochemical cells is significantly influenced by the DS and MW of NaCMC. We also showed a further influence impacting the electrode properties and cell performance, which are gel particles.

Notably, $\text{CMC}_{0.7, \text{low MW}}$ with a DS of 0.7 and low MW has shown the best results for the specific composition studied. High DS NaCMC leads to increased residual water and parasitic reactions, which worsen the cell performance. While lower DS shows reduced water content, electrodes suffer from higher electrical resistance. This leads to a reduced cell performance, overshadowing the benefit of less residual water. By increasing the MW, adhesion and interfacial resistance are improved, while the residual water content is significantly increased. This leads to an overall decrease of cell performance for electrodes using NaCMCs with high MW in comparison to their low MW counterparts, independent of the DS. Therefore, optimizing cell performance requires a careful balance between adhesion, resistivity, and residual water content. Despite the difference capacity-wise regarding high and low MW NaCMC, there is still a possible upside for higher MW. By delivering a high adhesion strength, it would be possible to further reduce the amount of NaCMC for the high MW polymers. By optimizing the electrode composition, the absolute amount of water would be reduced, due to the lower amount of water-absorbing binder being used. Therefore, a low molecular NaCMC cannot be substituted by a high MW NaCMC, without optimizing the composition of the electrode to achieve the same results.

Finally, it is essential to manage the amount of gel particles in the system to ensure optimal performance. A significant increase in the electrode properties is accomplished without any further change in the formulation. Additionally, by using a NaCMC with a low gel content, we showed that the rate capability and cell performance were significantly improved.

4. Experimental Section

Materials: The main focus of this investigation is on the influence of the DS, MW, and gel particles of NaCMC on electrode properties. If not stated differently, the following composition was used for all electrodes: 96 wt% of graphite (natural, MechanoCap 1P1, H.C. CARBON, Germany), 1.5 wt% of carbon black (CB, C-ENERGY Super C65, Imerys Graphite & Carbon, Switzerland), 1.25 wt% of SBR binder (TRD 2001, JSR Micro, Belgium), and 1.25 wt% of varying NaCMCs (IFF Speciality Products, Germany). Main properties of NaCMC like DS, MW, and gel particles are summarized in Table 1.^[16] Gel particle amount for the high MW was not included. It is important to note that suppliers produce NaCMC based on specific viscosity specifications rather than MW. For different DS, the MW had to be adapted to meet viscosity thresholds. As the intermolecular interaction between chains increases for lower DS, the MW for low DS NaCMCs is usually lower to meet said viscosity thresholds. This difference between NaCMCs for each molecular level was considered as less decisive.

Electrode Manufacturing: The slurry was mixed using a dissolver (Dispermat CA60, VMA Getzmann, Germany) with a 50 mm toothed disk in a batch container with a volume of 250 mL, while placed in a casing which was cooled by 20 °C water. NaCMC was dissolved in deionized water to create a 2 wt% solution first. Then the powder mixture of graphite and CB was continuously added. To add the premixed powder, a tip speed of 1.5 m s⁻¹ was applied. After the addition of the active material and CB was done, the tip speed was increased to 5 m s⁻¹ and stirred for 45 min. Finally, the tip speed was reduced to 1 m s⁻¹ to disperse the shear-sensitive SBR binder which was combined with the degassing at 100–200 hPa. The water content was adjusted to create a slurry with a solid content of 56 wt%. Electrodes were produced via roll-to-roll coating (KTFS, Mathis AG, Switzerland) with a doctor blade and a wet-film thickness of 75 μm. The two separate drying chambers had temperatures of 25 and 30 °C, while the coating was limited to a web speed of

Table 1. Summary for anode properties for varying DS and MW of the NaCMC.

Abbreviation ^{a)}	DS	MW [kDa]	No. of gel particles ^{b)}	Viscosity ^{c)} [mPa s]
CMC _{0.5, low MW}	0.5	290	10	2000
CMC _{0.7, low MW}	0.7	320	10	
CMC _{0.9, low MW}	0.9	360	25	
CMC _{0.5, high MW}	0.5	450	–	20 000
CMC _{0.7, high MW}	0.7	500	–	
CMC _{0.9, high MW}	0.9	630	–	
Gel ₁₀	0.7	320	10	2000
Gel ₁₀₀	0.7	320	100	
Gel ₂₅₀	0.7	320	250	

^{a)}The abbreviation depicts the DS and the MW of the NaCMC. The last abbreviation for gel particles depicts the amount of different gel particles in a NaCMC with the same polymer properties. ^{b)}Determined via visual assessment of a 25 cm² wet film.^[16] ^{c)}Viscosity of an aqueous 2 wt% NaCMC solution.

0.2 m min⁻¹. The anode slurries were coated on top of a copper current collector foil with a thickness of 10 μm. The areal capacity for all anodes was set at 2.1 ± 0.1 mAh cm⁻². To increase comparability, all coatings were calendared to a density of 1.1 g cm⁻³ equaling a porosity of 50% (GKL200, Saueressig, Germany). For the investigations of the influence of gel particle content, a new batch of copper foil was used.

5. Characterization

5.1. Electrode Properties

5.1.1. Adhesion Strength

First, the adhesion was measured by conducting a 90° peel-off test. Three 17 mm × 60 mm samples were measured. Each sample was pressed on the adhesive with 0.3 MPa for 10 s to enhance comparability. The sample was then placed in a zwickiLine Z2.5/TN (ZwickRoell, Germany), which pulled the sample at 600 mm min⁻¹ and moved the sample holder at the same rate to always allow for a 90° angle. The average force needed to peel off the electrode is the adhesion force of the respective sample, excluding the first and last 10 mm of the sample. All samples showed adhesive failure as their main mode of malfunction.

5.1.2. Electrical Resistance

To gain insights into the electrical resistance of the anode measurements via DC, 4-terminal method (RM2610 Electrode Resistance Measurement System, HIOKI, Japan) was performed. While measuring the volume resistivity, it also allowed to measure the interfacial resistance between the active material and collector. To determine statistics, measurements were repeated multiple times (N = 9). Locations were selected randomly. The term volume resistivity is equal to specific resistivity.

5.1.3. Residual Water Determined with Karl–Fischer

The residual water of the electrodes was determined by Karl–Fischer titration, via the Karl–Fischer oven. To prevent contamination of residue water of the vials, they were heated for 16 h at 120 °C under vacuum conditions. Furthermore, the carrier gas was dried via a molecular sieve before the residue was determined. The dried gas was then carrying residual water into the Karl–Fischer titration setup, where the moisture content was measured.

The Karl–Fischer titration was carried out in a dry room with a dew point of –60 °C. Electrode sheets were prepared as if used in a cell. They were densified to a porosity of 50% and dried for 16 h at 120 °C under vacuum conditions. The electrodes were cut into ≈30 mm × 100 mm samples, resulting in 180 mg anode material per sample, and put into the prepared vials. The sample chamber was then heated to a temperature of 160 °C for 12 min for the residue water to be extracted.

5.1.4. Gel Particle Determination via Wet Film

To determine the number of gel particles, the NaCMC solution was coated as a 100 μm film on top of a surface-treated

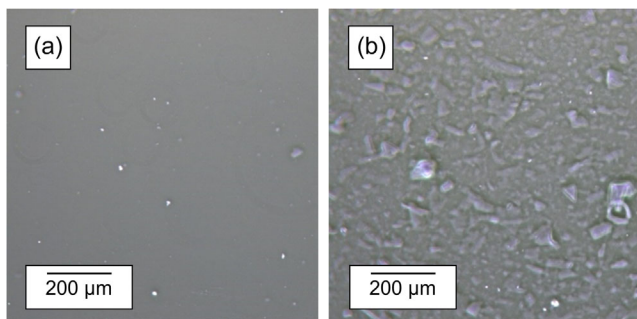


Figure 8. Visual assessment of two different NaCMC samples with a) low and b) high gel particle content.

polyethylene terephthalate surface, with a dimension of 5 by 5 cm resulting in a 25 cm² area. The wet coating of NaCMC solution then is observed under LED light, with gel particles being visually assessed as such.^[16] **Figure 8** shows two different NaCMC samples with (a) low and (b) high gel content, to illustrate visibility of the gel particles.

5.2. Electrochemical Characterization

5.2.1. Laboratory Pouch Cells

The investigations regarding varying MW and DS were investigated with pouch cells. All corresponding electrodes were dried for 16 h at 120 °C under vacuum conditions before they were assembled in a dry room with a dew point of −60 °C. An NMC(622) cathode with a mass loading of 12 mg cm^{−2} and a theoretical capacity of 175 mAh g^{−1} was used. The density of the electrode was constant at 2.7 g cm^{−3} with a cathode area of 25 cm² in the cell. The anode (29 cm²) was slightly overbalanced with an N/P ratio of 1.2. The N/P ratio refers to the relative electrode capacity of the negative (N) and positive (P) electrode in comparison to each other. The full cell setup was introduced into a pouch cell, where the electrodes were separated with a ceramic separator (33.4 cm², SEPARION, Degussa AG, Germany) while using an EC:DMC (1:1, Vol/Vol) electrolyte with 1 M of LiPF₆ dissolved (LP30, Sigma-Aldrich, USA). SEPARION is a commercial ceramic-coated (aluminum oxide) polyethylene terephthalate separator.^[15,17] For every electrode composition, a minimum of three pouch cells were built. To investigate the cycling behavior, the cells were connected to a BaSyTec (CTS-LAB, BaSyTec, Germany) system and stored in a climate chamber at 20 °C. Both formation and cycling were based on the theoretical capacity of the cathode (175 mAh g^{−1}). The rate capability test for discharge was first (0.5/0.5, 1/1, 1/2, 1/3, 1/5 C, constant current (CC) + constant voltage (CV) charge/CC discharge), which was concluded by long-term investigations for 1000 cycles (1 C CC CV charge/3 C CC discharge). Cut-off current for the CV step was set to 0.05 C.

Two 0.05 C steps were included every 200 cycles to investigate reversible and irreversible capacity loss during cycling. For comparability, three laboratory pouch cells were built per sample. Displayed capacities are the mean average of those three pouch cells.

5.2.2. Coin Cells

Here, anodes with NaCMC with different gel particle contents were used. Again, a full cell setup and the same NMC(622) cathodes with a mass loading of 12 mg cm^{−2} were used. Secondary drying of all electrodes consisted of 16 h at 120 °C under vacuum conditions before they were transferred into a glove box (200B, M.Braun Inertgas-Systeme GmbH, Germany) filled with argon gas (H₂O: <0.1 ppm, O₂: <0.1 ppm). The same cathode with an area of 1.13 cm² in the cell was used. The anode (1.13 cm²) was slightly overbalanced with an N/P ratio of 1.2. The full cell setup was introduced into a coin cell, where the electrodes were separated with a glass fiber separator (Whatman GF/C, Sigma-Aldrich, USA) while using an EC:DMC (1:1, Vol/Vol) electrolyte with 1 M of LiPF₆ dissolved (LP30, Sigma-Aldrich, USA). Both formation and cycling were based on the theoretical capacity of the cathode (175 mAh g^{−1}). The discharge rate capability test was the same as for the pouch cells while the long-term investigations were reduced to 200 cycles (3 C CC discharge/1 C CC CV charge). Cut-off current for the CV step was set to 0.05 C. For comparability three coin cells were built per sample. Displayed capacities are the mean average of those three coin cells.

Acknowledgements

This work contributes to the research performed at CELEST (Center for Electrochemical Energy Storage Ulm Karlsruhe) and Material Research Center for Energy Systems (MZE).

Conflict of Interest

The authors declare no conflict of interest.

Author Contributions

Noah Keim: conceptualization (lead); data curation (lead); formal analysis (lead); investigation (lead); methodology (lead); validation (lead); visualization (lead); writing—original draft (lead); writing—review & editing (lead). **Andreas Weber:** conceptualization (supporting); data curation (supporting); investigation (supporting); writing—review & editing (equal). **Marcus Müller:** conceptualization (equal); formal analysis (equal); writing—review & editing (equal). **Ulrike Kaufmann:** conceptualization (equal); data curation (supporting); investigation (supporting); writing—review & editing (supporting). **Werner Bauer:** formal analysis (supporting); funding acquisition (lead); project administration (equal); supervision (equal); writing—review & editing (equal). **Oliver Petermann:** conceptualization (equal); formal analysis (equal); writing—review & editing (supporting). **Roland Bayer:** conceptualization (equal); formal analysis (equal); writing—review & editing (supporting). **Helmut Ehrenberg:** conceptualization (equal); project administration (equal); resources (lead); supervision (equal); writing—review & editing (equal).

Data Availability Statement

The data that support the findings of this study are available from the corresponding author upon reasonable request.

Keywords

electrode processing, electrode properties, gel particles, impurities, lithium-ion batteries, sodium carboxymethylcellulose

Received: November 4, 2024

Revised: February 13, 2025

Published online:

- [1] a) H. K. Amusa, M. Sadiq, G. Alam, R. Alam, A. Siefan, H. Ibrahim, A. Raza, B. Yildiz, *J. Mater. Cycles Waste Manage.* **2024**, *26*, 1959; b) J. Duan, X. Tang, H. Dai, Y. Yang, W. Wu, X. Wei, Y. Huang, *Electrochem. Energy Rev.* **2020**, *3*, 1; c) F. Zou, A. Manthiram, *Adv. Energy Mater.* **2020**, *10*, 2002508.
- [2] a) L. Zhang, X. Wu, W. Qian, K. Pan, X. Zhang, L. Li, M. Jia, S. Zhang, *Electrochem. Energy Rev.* **2023**, *6*, 36; b) Z. Zhang, T. Zeng, Y. Lai, M. Jia, J. Li, *J. Power Sources* **2014**, *247*, 1.
- [3] a) Y.-B. Wang, Q. Yang, X. Guo, S. Yang, A. Chen, G.-J. Liang, C.-Y. Zhi, *Rare Met.* **2022**, *41*, 745; b) V. A. Nguyen, C. Kuss, *J. Electrochem. Soc.* **2020**, *167*, 065501.
- [4] a) D. Bresser, D. Buchholz, A. Moretti, A. Varzi, S. Passerini, *Energy Environ. Sci.* **2018**, *11*, 3096; b) J.-H. Lee, S. Lee, U. Paik, Y.-M. Choi, *J. Power Sources* **2005**, *147*, 249.
- [5] J. Drogenik, M. Gaberscek, R. Dominko, F. W. Poulsen, M. Mogensen, S. Pejovnik, J. Jamnik, *Electrochim. Acta* **2003**, *48*, 883.
- [6] a) A. Berardi, P. H. M. Janssen, B. H. J. Dickhoff, *J. Drug Del. Sci. Tech.* **2022**, *70*, 103261; b) R. C. Rowe, R. C. Rowe, P. J. Sheskey, S. C. Owen, A. American Pharmacists, *Handbook of Pharmaceutical Excipients*, 5th ed., Pharmaceutical Press, London, UK **2005**; c) P. Zampieri, T. Flanagan, E. Meehan, J. Mann, N. Fotaki, *Eur. J. Biomed. Pharm. Sci.* **2017**, *111*, 1.
- [7] a) R. Jagau, F. Huttner, J. K. Mayer, H. Cavers, S. Scheffler, J. Brokmann, A. Kwade, *Energy Technol.* **2023**, *11*, 2200871; b) F. Ma, Y. Fu, V. Battaglia, R. Prasher, *J. Power Sources* **2019**, *438*, 226994; c) J. M. Torres, C. M. Stafford, B. D. Vogt, *Polymer* **2010**, *51*, 4211.
- [8] S. Koumarios, R. Kaiyum, C. J. Barrett, N. Madras, O. Mermut, *Phys. Chem., Chem. Phys.* **2021**, *23*, 300.
- [9] W. Bauer, F. A. Çetinel, M. Müller, U. Kaufmann, *Electrochim. Acta* **2019**, *317*, 112.
- [10] J. Entwistle, R. Ge, K. Pardikar, R. Smith, D. Cumming, *Renewable Sustainable Energy Rev.* **2022**, *166*, 112624.
- [11] D. Burger, N. Keim, J. Shabbir, Y. Gao, M. Müller, W. Bauer, A. Hoffmann, P. Scharfer, W. Schabel, *Energy Technol.* **2024**, 2401668.
- [12] a) J. H. Elliot, A. J. Ganz, *Rheol. Acta* **1974**, *13*, 670; b) C. G. Lopez, R. H. Colby, J. T. Cabral, *Macromolecules* **2018**, *51*, 3165; c) C. G. Lopez, S. E. Rogers, R. H. Colby, P. Graham, J. T. Cabral, *J. Polym. Sci., Part B* **2015**, *53*, 492.
- [13] a) D. J. Yang, X. J. Li, N. N. Wu, W. H. Tian, *Electrochim. Acta* **2016**, *188*, 611; b) F. Huttner, W. Haselrieder, A. Kwade, *Energy Technol.* **2020**, *8*, 1900245; c) U. Langklotz, M. Schneider, A. Michaelis, *J. Ceram. Sci. Technol.* **2013**, *4*, 69.
- [14] A. Weber, N. Keim, A. Gyulai, M. Mueller, F. Colombo, W. Bauer, H. Ehrenberg, *J. Electrochem. Soc.* **2024**, *171*, 040523.
- [15] A. Smith, P. Stüble, L. Leuthner, A. Hofmann, F. Jeschull, L. Mereacre, *Batter. Supercaps* **2023**, *6*, e202300080.
- [16] T. Klamet, DDP Specialty Products Germany GmbH & Co. KG **2023**.
- [17] S. S. Zhang, *J. Power Sources* **2007**, *164*, 351.